Düzce University Journal of Science & Technology

Research Article

Electric and Magnetic Field Analysis for a 34.5 kV Transformer Under Composite Voltage Conditions: COMSOL Multiphysics Simulation

Emre TUNÇ [a,*], Murat FİDAN [a]

[a] *Department of Electrical and Electronics Engineering, Faculty of Engineering, Bolu Abant Izzet Baysal University, Bolu, TÜRKİYE*

* *Corresponding author's e-mail address: emretunc@ibu.edu.tr*

DOI: 10.29130/dubited.1624167

ABSTRACT

Transformers are one of the basic components of electrical power systems and play a critical role in energy conversion. However, overvoltages and environmental stresses can cause failures in transformer insulation systems. These failures can negatively affect reliability by reducing the lifetime of insulation systems and can lead to serious losses in power transmission. Moreover, sudden failures increase economic costs and reduce the overall efficiency of power systems. For this reason, a 3 MVA, 34.5 kV dry-type distribution transformer was modeled using COMSOL Multiphysics software. Based on IEC 60076-3 and IEC 60060-1:2010 standards, a lightning impulse voltage with an amplitude of 170 kV and nominal operating voltage were simultaneously applied to the modeled transformer. Electric field strength, magnetic flux density, and electric potential distributions were analyzed under composite voltage conditions. Under these conditions, the effects of electrical stress on the insulation strength are discussed in detail. The results obtained show the negative effects of composite voltage signal components on the insulation performance of the transformer and potential areas for improvement.

Keywords: *Composite voltage, electric field analysis, magnetic flux density, COMSOL Multiphysics, lightning impulse voltage*

Kompozit Gerilim Koşulları Altında 34,5 kV' luk Transformatörün Elektrik ve Manyetik Alan Analizi: COMSOL Multiphysics Simülasyonu

ÖZ

Transformatörler, elektrik güç sistemlerinin temel bileşenlerinden biri olup enerji dönüşümünde kritik bir rol oynamaktadır. Ancak, aşırı gerilimler ve çevresel zorlanmalar, transformatörlerin yalıtım sistemlerinde arızalara yol açabilmektedir. Bu arızalar, yalıtım sistemlerinin ömrünü kısaltarak güvenilirliği olumsuz yönde etkileyebilir ve enerji iletiminde ciddi kayıplara yol açabilir. Ayrıca, ani arızalar ekonomik maliyetleri artırırken, güç sistemlerinin genel verimliliğini de düşürmektedir. Bu sebeple, çalışma kapsamında 3 MVA gücünde, 34,5 kV'luk kuru tip bir dağıtım transformatörü, COMSOL Multiphysics yazılımı kullanılarak modellenmiştir. IEC 60076-3 ve IEC 60060-1:2010 standartları temel alınarak, modellenen transformatöre genliği 170 kV olan yıldırım darbe gerilimi ile

Received: 21/01/2025, Revised: 02/05/2025, Accepted: 07/05/2025

nominal işletme gerilimi eş zamanlı olarak uygulanmıştır. Karma gerilim koşulları altında elektrik alan şiddeti, manyetik akı yoğunluğu ve elektrik potansiyeli dağılımları analiz edilmiştir. Bu koşullar altında yalıtım sistemlerinde meydana gelen elektriksel zorlanmanın yalıtım dayanımı üzerindeki etkileri ayrıntılı olarak ele alınmıştır. Elde edilen sonuçlar, karma gerilim işareti bileşenlerinin transformatörün yalıtım performansı üzerindeki olumsuz etkilerini ve potansiyel iyileştirme alanlarını ortaya koymaktadır.

Anahtar Kelimeler: *Karma gerilim, elektrik alan analizi, manyetik akı yoğunluğu, COMSOL Multiphysics, yıldırım darbe gerilimi*

I. INTRODUCTION

Transformers are critical devices to ensure energy conversion in electrical power systems and to realize the transmission of electrical energy efficiently. Transformers, which play a critical role in the generation, transmission, and distribution stages of electrical energy, are among the main components of the electrical power system. Efficient operation of transformers is of great importance to reduce energy losses and increase system reliability. However, these devices are subjected to various electrical and mechanical stresses during their operational life, which increases the probability of failure [1, 2].

Surge overvoltages caused by lightning discharges, switching events, and insulation failures are some of the most common conditions that can cause faults in electrical power systems [3]. Overvoltages damage the insulation of devices, causing arcing and short-circuit currents [4]. The insulation of energy transmission systems is especially stressed due to transient overvoltages [5]. Switching-induced overvoltages can cause inter-phase faults in electrical equipment and degradation of insulation systems [6]. Lightning discharges can cause economic losses and equipment failures in power systems [7]. In transformers, which are widely used in electrical power systems, one of the main causes of failures is degradation in the insulation system. Insulation failures are caused by various factors such as high electric field intensity, moisture accumulation, thermal aging, and dielectric breakdowns in the insulation material. Such failures negatively affect energy conversion processes and reduce system reliability [8]. In addition to insulation failures, other problems such as partial discharges and arcing are among the main factors that negatively affect the performance of transformers.

The effects of harmonic voltages on the insulation material are associated with partial discharge behaviors in transformers [9]. These partial discharges usually occur at micro-gaps, surfaces, or geometrical irregularities in the insulation material. This process can result in irreversible damage to the insulation structure and severely reduce the transformer's lifetime. Electrical stress due to ionization increases the risk of failure by straining the dielectric strength of the insulation, especially in high voltage applications [9, 10].

The IEC 60076-3 standard includes the testing of transformers under a lightning impulse voltage with a characteristic of 1.2/50 μs and the evaluation of the effects of this impulse voltage on the transformer [11]. The effects of overvoltages on the electric field and potential distribution within windings is a topic that continues to be extensively researched today. Electric field concentrations cause localized weakening of the insulating material and hence the initiation of partial discharges. This process weakens the dielectric strength of the insulating material, threatening the performance and safety of the device [10].

The short-term but high amplitude effects of lightning impulses can cause permanent deformations and performance losses in transformer insulation systems. In addition, the total strain caused by transient overvoltages combined with the operating voltage forces the dielectric strength limits of the insulation material and increases failure rates. The costly repairs and power outages caused by such events require further research to ensure the safe and efficient operation of transformers.

Although there are studies in the literature on electric field and magnetic field analysis of transformers, transformer analysis under composite voltage is a subject that needs to be researched in the literature. In recent years, there has been a growing number of studies focusing on the modeling of the electromagnetic characteristics of transformers using various analytical methods. In the study conducted by Özüpak et al. [12], magnetic behaviors were evaluated through the combined use of the Finite Element Method (FEM) and Artificial Neural Networks (ANN). These approaches highlight the increasing significance of numerical analyses in accurately modeling transformer performance. In another study [13], the effects of subharmonics on electromagnetic behavior and losses in transformers were investigated using the FEM, and the importance of numerical analyses in transformer performance modeling was emphasized.

In the literature, electromagnetic analyses of transformers are generally carried out using FEM-based software such as ANSYS Maxwell and COMSOL. In the study by Özüpak [10], the effects of lightning impulse voltage on the winding insulation of a 15 MVA dry-type transformer were analyzed using ANSYS Maxwell. Similarly, Hu et al. [14] conducted an electric field distribution analysis of a 110 kV transformer using COMSOL. Unlike previous works, this study investigates the behavior of a 34.5 kV transformer under composite voltage (AC + impulse) conditions, which have been studied to a limited extent in the literature, and analyzes both magnetic flux density and electric field distribution simultaneously.

In addition to these studies that examine the effect of impulse voltage on transformers, there are other studies in the literature on electric field analysis under composite voltage.

Ispirli et al. [15] analyzed the electric field distribution of silicone rubber insulators used at 66 kV and 110 kV voltage levels by the finite element method. The study was carried out under composite voltage consisting of AC and DC. Yazıcı et al. [16] investigated the effect of composite voltages on the disconnector in terms of electrical stress. In Comsol Multiphysics software, the electric field and electric potential distribution of a 170 kV disconnector under composite voltage consisting of AC and impulse voltage components were analyzed.

In addition to the aforementioned electromagnetic analysis studies, the importance of accurate thermal modeling in transformer design has also been emphasized in the literature. Seddik et al. [17] performed a comprehensive 2D and 3D thermal analysis of power transformers using the Finite Element Method, emphasizing the significance of temperature distribution on transformer reliability. Likewise, Tsili et al. [18] conducted a coupled 3D thermal-fluid analysis of power transformers to evaluate internal cooling mechanisms and their effects on hot spot temperatures. These studies emphasize that combining electromagnetic and thermal field analyses is essential for designing reliable and efficient transformers.

The effects of composite voltages on transformers, especially electrical stress and potential distribution, have been discussed in a limited way in the literature. Therefore, the electric field distribution and potential effects of composite voltages on the transformer need to be studied in more detail. This study aims to comprehensively investigate the electric and magnetic field effects of composite voltages on transformers. In particular, the electrical stress and potential changes in transformer insulation systems caused by composite voltages consisting of AC and impulse voltage components have been investigated. The results of the COMSOL Multiphysics-based analysis contribute to the development of reliable and durable insulation solutions in transformer design. This study is expected to provide a better understanding of the effects of composite voltages on transformers and provide benefits to improve the safety of power systems. Unlike earlier studies that examined either AC or impulse voltage effects in isolation, this study provides a unified analysis under composite voltage conditions by combining both waveform components simultaneously. The developed model not only includes realistic time-domain waveform definitions, but also incorporates the nonlinear B-H characteristics of the transformer core, providing a more accurate estimation of the electromagnetic behavior under real-world conditions. Furthermore, the voltage profiles used in the simulations are based on IEC 60076-3 and IEC 60060-1:2010 standards, enhancing the reliability and applicability of the model [11, 19]. These aspects

distinguish this work from prior studies and underline its novelty in the context of transformer insulation evaluation.

II. COMPOSITE VOLTAGES

Electrical power system components can be exposed not only to the operating voltage but also to different voltage components [15]. Composite voltages consisting of AC and DC [20, 21] or AC and impulse voltage [16, 22] can stress the insulation performance of the devices in the electrical power system different from the nominal operating conditions. If the insulation performance of the devices in the power system is stressed differently from the nominal operating conditions, it may increase the risk of failure. Therefore, testing of electrical power system components under composite voltages is critical for both verifying design criteria and determining the limits of insulation systems [16, 23].

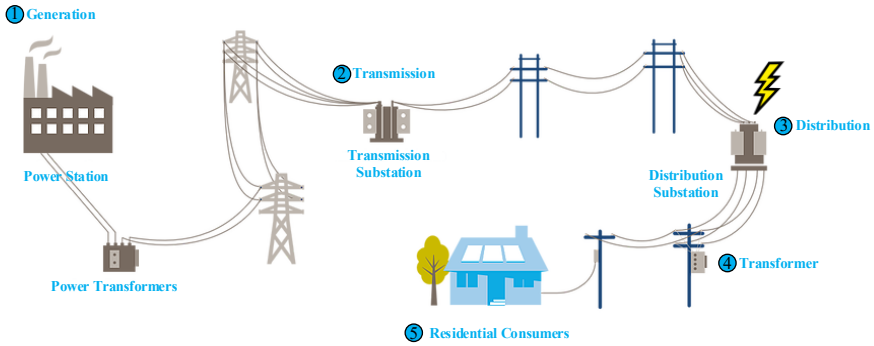

Figure 1. *Lightning impulse voltage caused by external overvoltage in an electrical power system.*

The IEC 60060-1:2010 standard specifies the basic methods and criteria for testing under composite voltages [19]. According to this standard, the voltage components that constitute the composite voltage should be characterized by the voltage value and time delay parameters. Figure 2 shows the voltage and time delay parameters of the composite voltage components according to IEC 60060-1:2010. In Figure 2, Δt is the time delay parameter and U+ and U- are the amplitude of the voltage components.

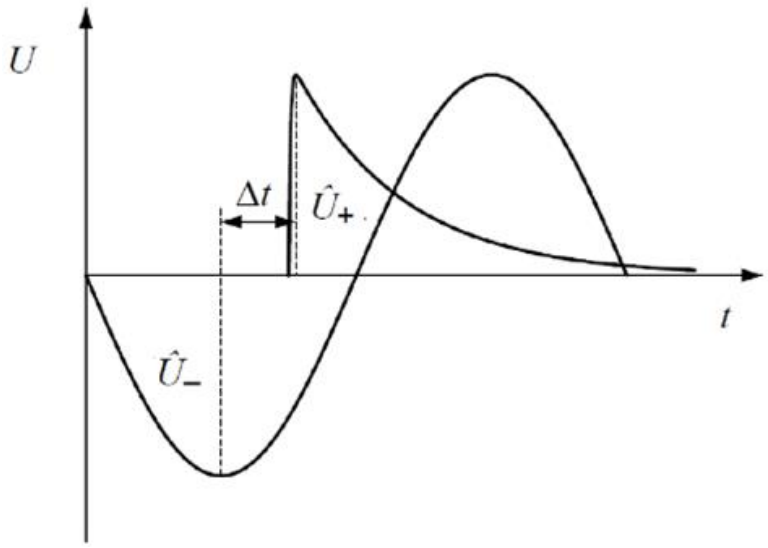

Figure 2. *Voltage and time delay parameters of composite voltage components according to IEC 60060-1:2010 standard [19].*

Lightning impulse voltages are used to test the insulation performance of power systems and to assess the reliability of equipment [24, 25]. The IEC 60060-1:2010 standard defines in detail the characteristics and application methods of the lightning impulse voltage signal. The standard lightning impulse voltage is defined by four parameters, Um peak value, T1 front time, T2 tail time, and polarity [26, 27]. Figure 3 shows the standard lightning impulse voltage signal with these parameters.

For a standard lightning impulse voltage with 1.2/50 µs characteristic, the value of 1.2 µs refers to the front time of the waveform and 50 µs refers to the time to 50% of the peak value. According to these values, the amplitude of the impulse voltage increases rapidly and decreases slowly with time.

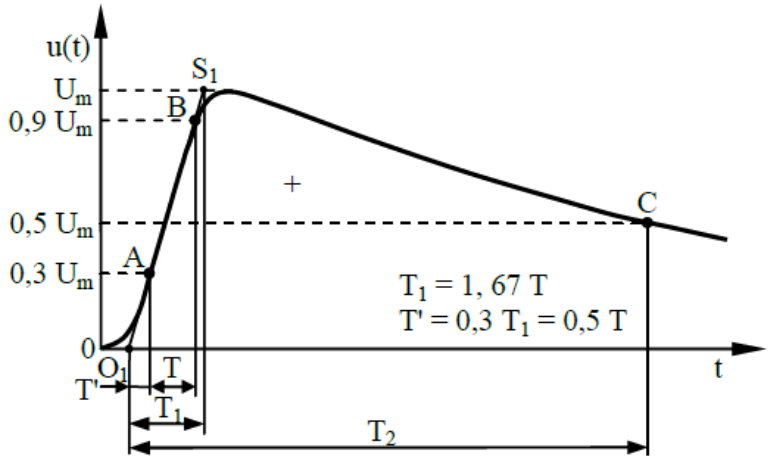

Figure 3. *Lightning impulse voltage signal according to IEC 60060-1:2010 standards [28].*

III. SIMULATION STUDY

This section presents a simulation study to investigate the behavior of transformer insulation systems under lightning impulse voltages and composite voltages. In the study, the electric field distribution, potential concentrations, and magnetic flux density in the insulation system were analyzed in detail using COMSOL Multiphysics software. The Magnetic Fields module (AC/DC Module) was employed for magnetic flux density analysis, while the Electrostatics module was used for electric field distribution studies.

In the present study, a 3 MVA dry-type distribution transformer with a mantel core structure was modeled and analyzed under composite voltage. The transformer geometry was created based on a shell-type core structure using the built-in CAD tools of COMSOL. Key components such as the core, primary and secondary windings, and surrounding air domain were modeled in 3D. The dimensions were selected based on typical design values for medium-voltage dry-type distribution transformers. The structural features and geometrical dimensions of the model are presented in Figure 4. The parameter values of the designed transformer are given in Table 1. Tetrahedral elements were used for meshing the model, with a maximum element size of 5 mm.

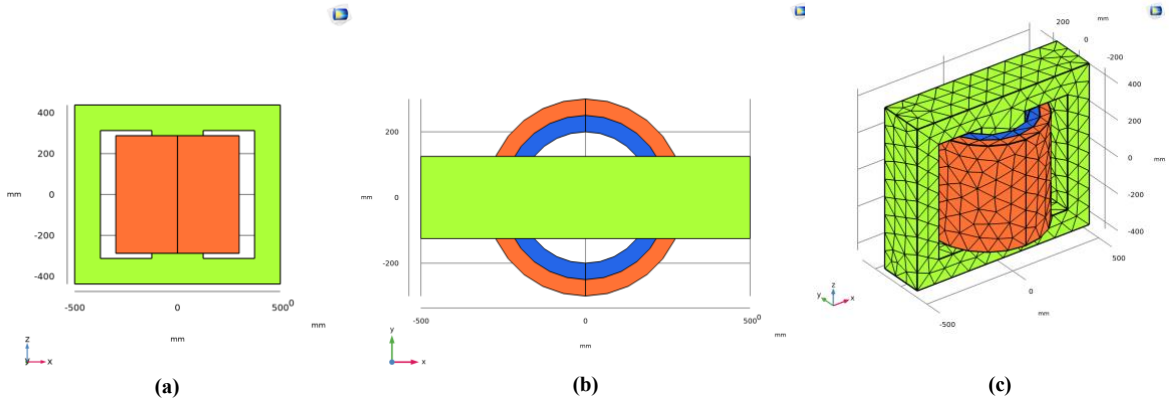

***Figure* 4.** *The designed transformer; (a) front view, (b) top view, (c) mesh model.*

The magnetic core was modeled using a nonlinear B-H curve to accurately represent the saturation behavior of the laminated core steel. The core of the transformer was modeled in the software environment by considering the B-H curve and sheet metal properties of the magnetic material. Insulating regions were modeled using dielectric constants of $\varepsilon_r = 4$, corresponding to epoxy resin-based insulation. Copper was used for the winding material with standard conductivity and relative permeability values. The magnetic B-H curve of the core material used in the design is presented in Figure 5.

Table 1. *Parameter values of the designed transformer*

Parameters	Values
Rated Power	3 MVA
Primary Voltage	34.5 kV
Secondary Voltage	400 V
Frequency	50 Hz

The analysis of the modeled transformer was carried out under nominal operating conditions and lightning impulse voltage. For this purpose, AC and lightning impulse voltage were applied simultaneously to the high voltage windings of the transformer in COMSOL Multiphysics software. Figure 6 (a) illustrates the time variation of the nominal operating voltage applied to the transformer windings. The frequency of the nominal operating voltage is 50 Hz and the amplitude is 34.5 kV.

The lightning impulse voltage required to analyze the transformer under composite voltage in the COMSOL Multiphysics software was generated in the MATLAB/Simulink environment and imported into COMSOL Multiphysics. The time dependent variation of the lightning impulse voltage signal generated in MATLAB/Simulink environment is given in Figure 6 (b). The impulse voltage in Figure 6 (b) has a front time of 1.2 µs and a tail time of 50 µs. The transient behavior of the composite voltage signal was analyzed using a time-dependent solver; considering the IEC 60060-1:2010 standard [19], the total simulation time was set to 50 ms and the time step to 0.1 µs in order to accurately resolve the fast-rising front of the impulse voltage component. In the COMSOL Multiphysics environment, a relative tolerance of 10^{-4} was selected to ensure numerical accuracy during the transient analysis. To confirm the reliability of the simulation, sensitivity analyses were conducted by varying the time step and mesh resolution. The observed variation in peak field values was found to be less than 2%, ensuring statistical consistency in the obtained data.

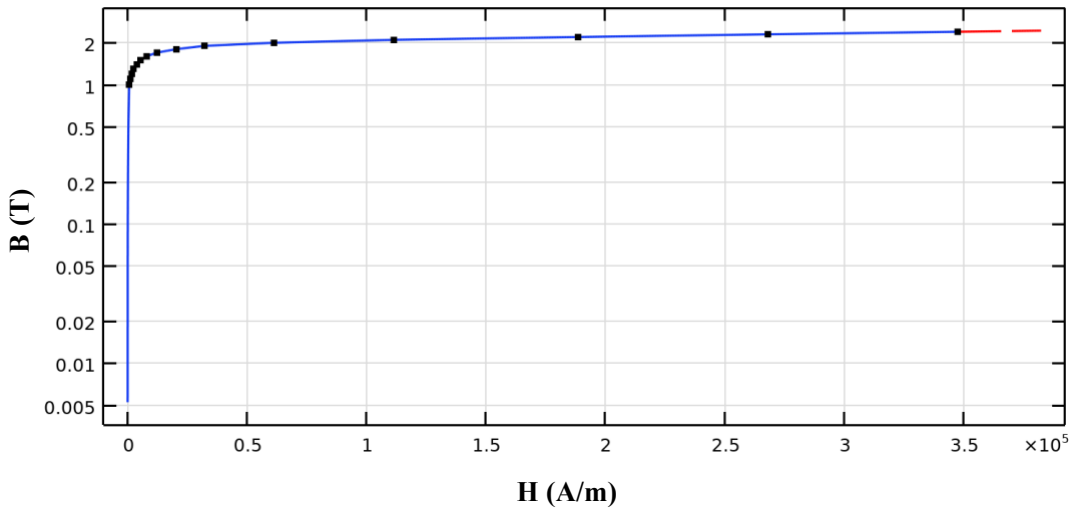

***Figure* 5.** *B-H curve of the core used in transformer design.*

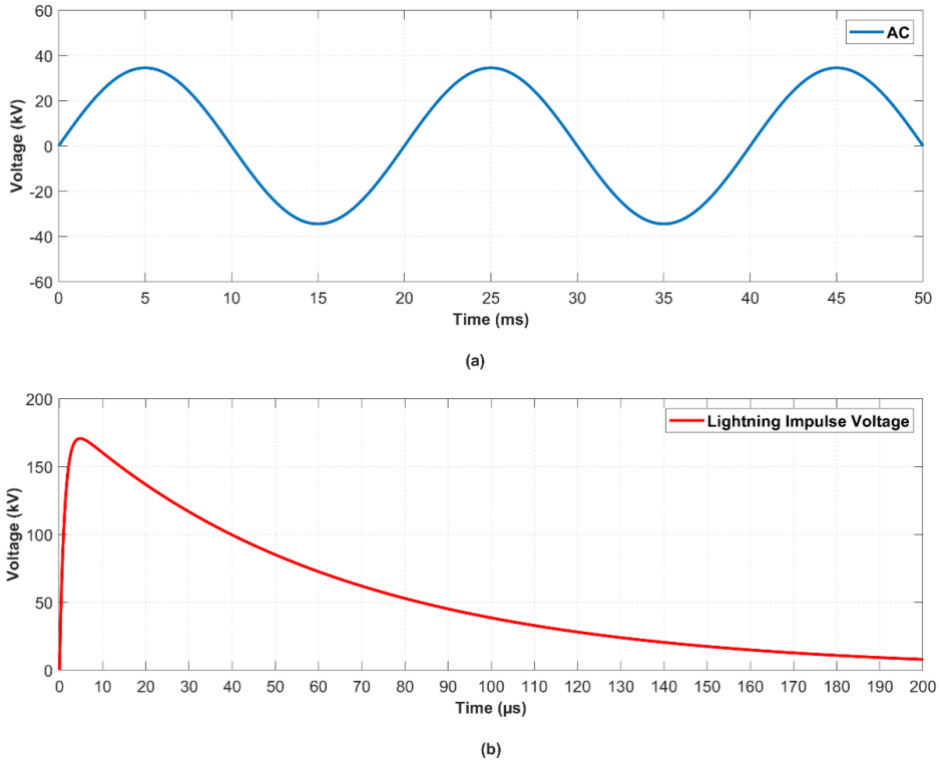

***Figure* 6.** *Applied to the windings of the transformer; (a) nominal operating voltage, (b) lightning impulse voltage with 1.2/50 µs standard.*

For the analysis of the designed transformer under composite voltage, a positive impulse at positive half-cycle, positive impulse at negative half-cycle, negative impulse at positive half-cycle, and negative impulse at negative half-cycle signals are generated. Figure 7 presents the AC (nominal operating voltage) signal as well as the positive and negative impulse voltage signals.

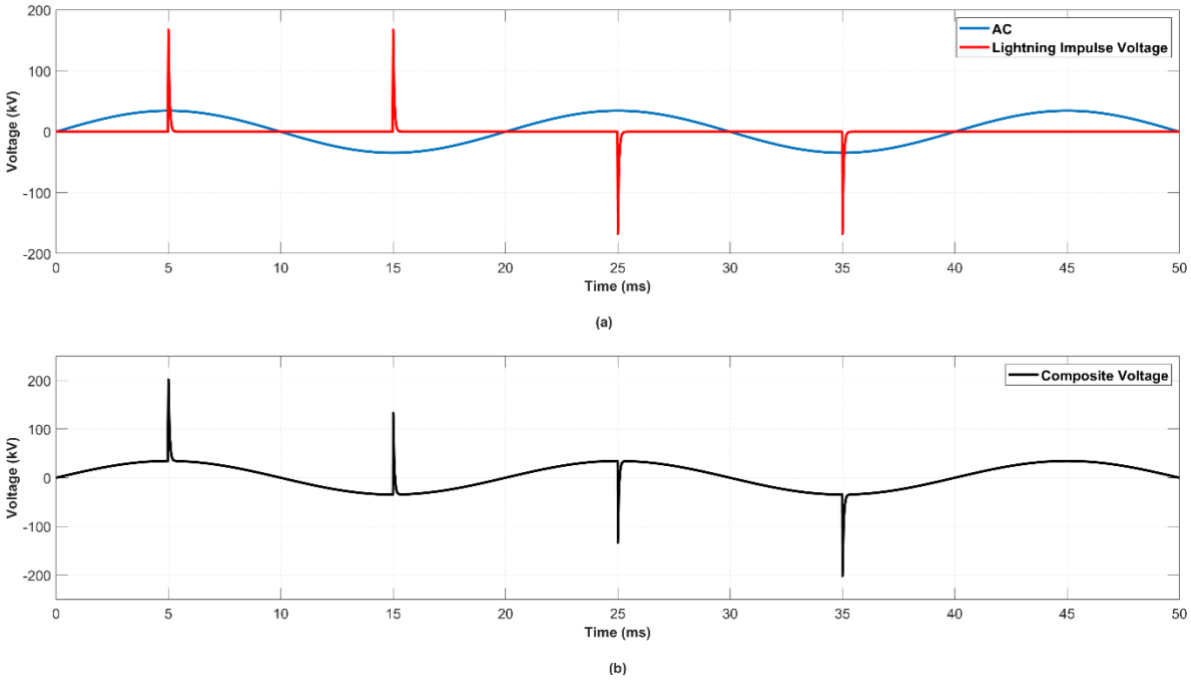

Figure 7. *Generated in MATLAB/Simulink environment; (a) AC and lightning impulse voltage, (b) composite voltage.*

Faults caused by lightning impulse voltages in electrical power systems vary depending on the timing of the impulse application and the amplitude of the operating voltage. Such voltages can impact the power system at any phase of the operating voltage, leading to faults of varying severity. To evaluate the most critical scenarios, this study examines the application of positive and negative lightning impulse voltages at the positive and negative peaks of the AC waveform. Positive impulse voltages with a peak value of 170 kV, as specified in the IEC 60076-3 standard, were applied to the designed transformer at 4.9988 ms and 14.9988 ms, as shown in Figure 7 (a) [19]. Similarly, negative impulse voltages with a peak value of 170 kV were applied at 24.9988 ms and 34.9988 ms, respectively.

The AC and lightning impulse voltage signals in Figure 7 (a) are superimposed to obtain a composite voltage for the analysis of the transformer. For the analysis of the transformer, the lightning impulse voltage signal was superimposed on the AC signal with a period of 50 ms. The lightning impulse voltage was applied at the positive half-cycle (t=4998.8 µs and t=24998.8 µs) and negative half-cycle (t=14998.8 and t=34998.8 µs) of the AC. The composite voltage signal generated in MATLAB/Simulink to be applied to the transformer for analysis in COMSOL Multiphysics is given in Figure 7 (b).

A. SIMULATION STUDY RESULTS

In this section, the results of the magnetic and electric field analysis of the transformer designed using COMSOL Multiphysics software under composite voltage are presented. The transformer is analyzed under nominal operating voltage and impulse voltage; magnetic flux density, electric field distribution, and electric potential distribution are analyzed in detail.

The composite voltage signal shown in Figure 8 was applied to the high voltage windings of the modeled transformer in COMSOL Multiphysics software.

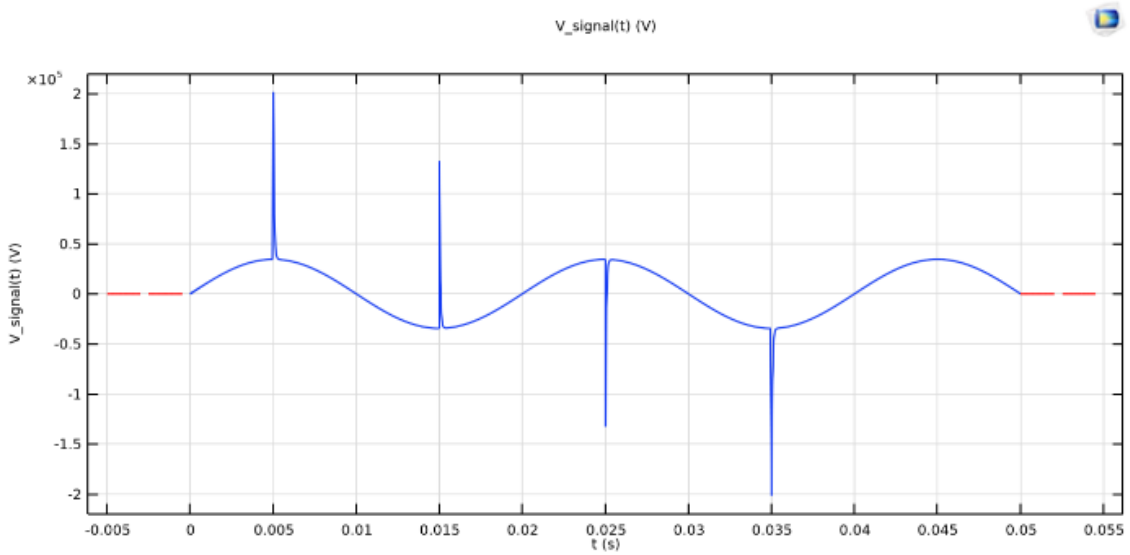

***Figure* 8.** *Composite voltage signal applied to the high voltage windings of the transformer in COMSOL Multiphysics software.*

The magnetic flux density distribution obtained for t=5 ms of the composite voltage signal applied to the high voltage windings of the designed transformer is given in Figure 9. The maximum value of the magnetic flux density is obtained as 1.82353 T for this moment when the positive impulse voltage reaches its peak value at the positive half-cycle of the nominal operating voltage.

The distribution of the electric field and electric potential at t=5 ms are shown in Figure 10. At the peak of the positive lightning impulse voltage, the maximum electric field strength was determined to be 78436.2 V/m. The electric potential distribution in the transformer volume increased on the windings as can be seen in Figure 10 (c).

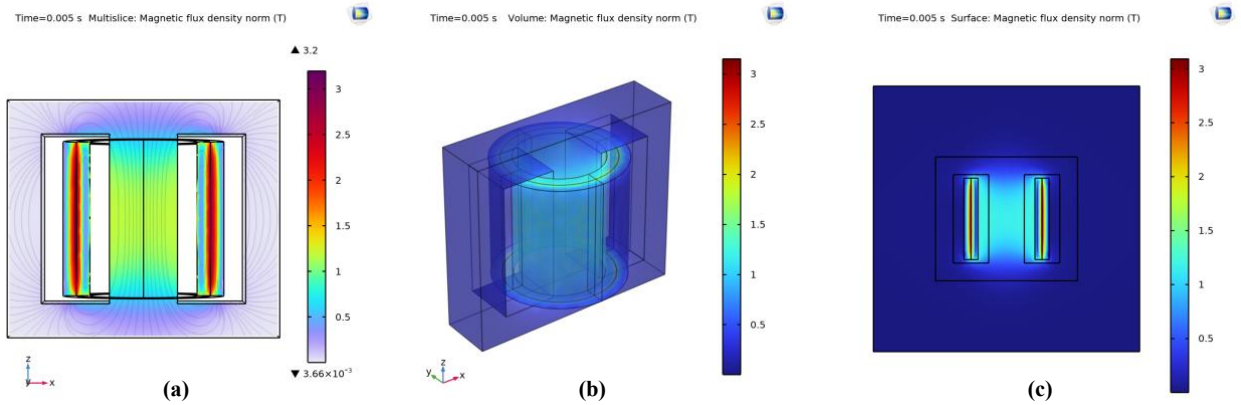

***Figure* 9.** *Magnetic flux density obtained at t=5ms: (a) in the cross-section, (b) in the volume, (c) on the surface.*

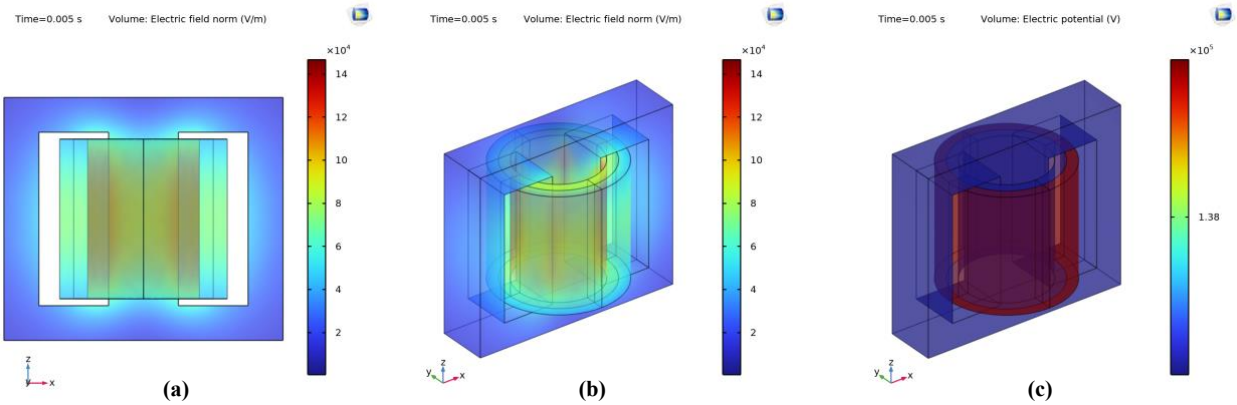

***Figure* 10.** *(a) electric field distribution (xz plane view), (b) electric field distribution (isometric view), (c) electric potential distribution obtained for t=5 ms.*

The magnetic flux density distribution obtained for t=15 ms of the composite voltage signal is given in Figure 11. The magnetic flux density is 1.60468 T for this time when the peak value of the negative impulse voltage is obtained in the negative half-cycle of the AC.

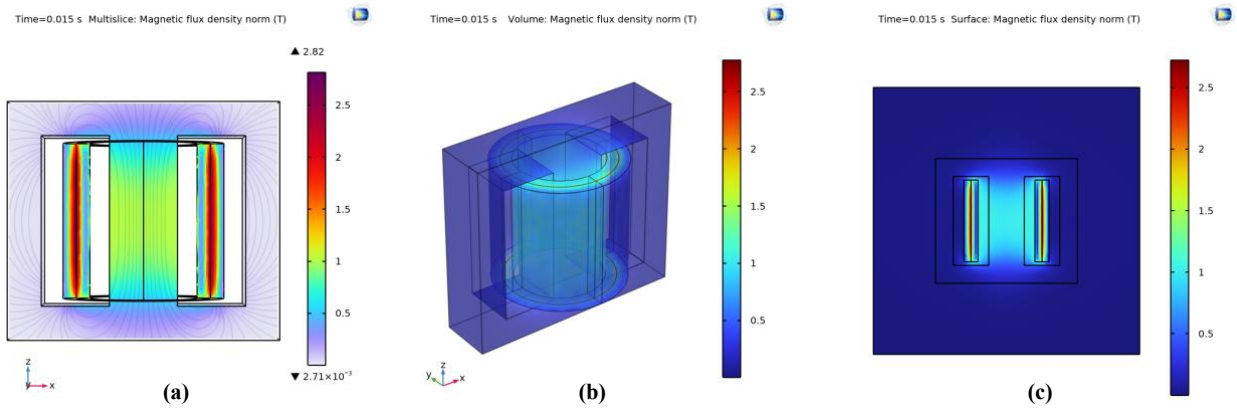

***Figure* 11.** *Magnetic flux density obtained at t=15ms: (a) in the cross-section, (b) in the volume, (c) on the surface.*

The electric field and electric potential distribution obtained for t=15 ms are shown in Figure 12. The amplitude of the electric field strength and potential distribution obtained for the moment t=15 ms due to the positive impulse voltage at the negative half-cycle of the nominal operating voltage is smaller than the values obtained for t=5 ms. The maximum electric field strength for t=15 ms is 42343.2 V/m and the maximum electric potential on the transformer is 69469.1 V.

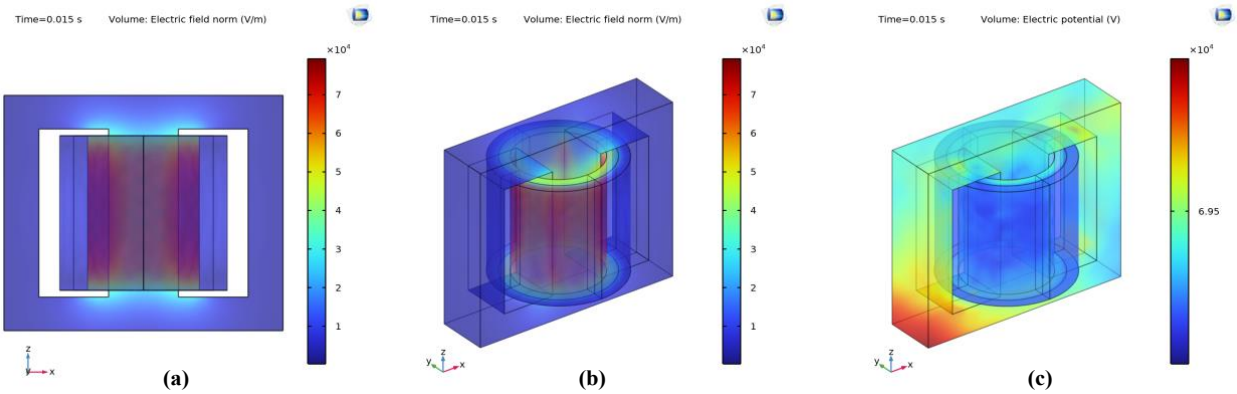

***Figure* 12.** *(a) electric field distribution (xz plane view), (b) electric field distribution (isometric view), (c) electric potential distribution obtained for t=15 ms.*

Figure 13 shows the magnetic flux density in the transformer volume at 25 ms when the negative impulse signal is applied at the positive half-cycle of the AC and the composite voltage reaches its peak value. The maximum magnetic flux density generated by the composite voltage signal in the transformer volume at this time is 1.59325 T.

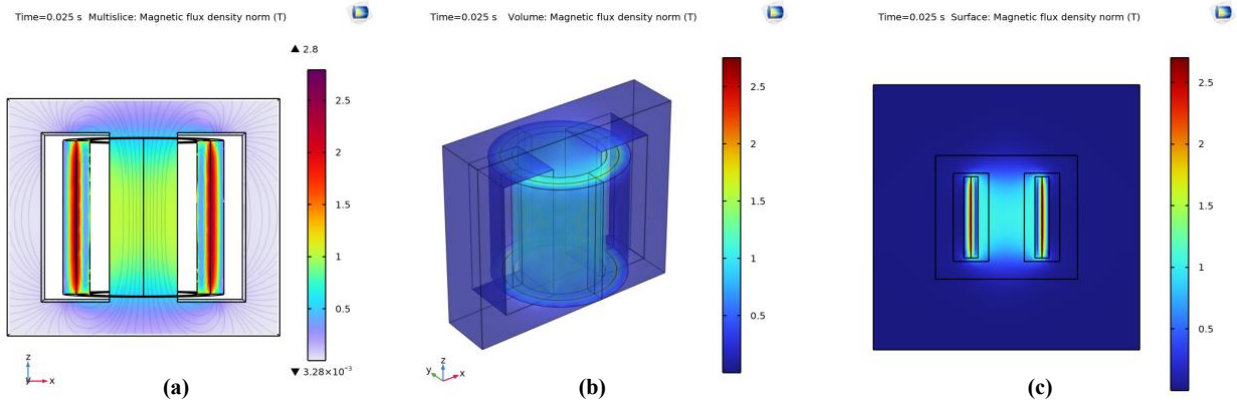

Figure 13. *Magnetic flux density obtained at t=25ms: (a) in the cross-section, (b) in the volume, (c) on the surface.*

The electric field and electric potential distribution of the composite voltage signal for t=25 ms are shown in Figure 14. At the moment of the peak value of the negative lightning impulse voltage, the maximum amplitude of the electric field strength was 39690.8 V/m. Due to the negative impulse voltage in the positive half-cycle, a negative electric field strength was formed in the transformer volume.

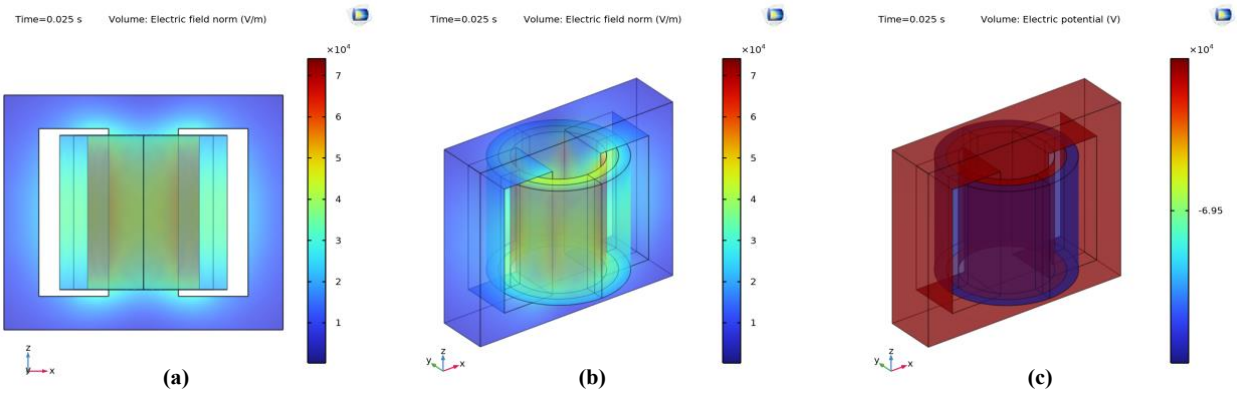

Figure 14. *(a) electric field distribution (xz plane view), (b) electric field distribution (isometric view), (c) electric potential distribution obtained for t=25 ms.*

The magnetic flux density distribution at t=35 ms for the composite voltage signal is shown in Figure 15. For t= 35 ms at the negative half-cycle of the operating voltage, the magnetic flux density is obtained as 1.86759 T.

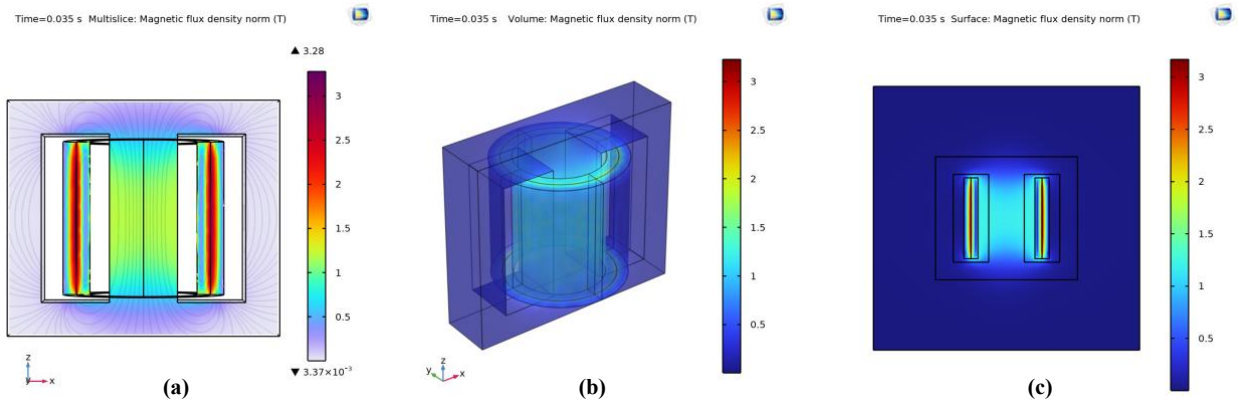

Figure 15. *Magnetic flux density obtained at t=35ms: (a) in the cross-section, (b) in the volume, (c) on the surface.*

The electric field and electric potential distribution obtained for t=35 ms of the composite voltage signal are shown in Figure 16. At the negative half-cycle of the operating voltage, the maximum amplitude of the electric field strength is 79481.2 V/m for t=35 ms of the composite voltage.

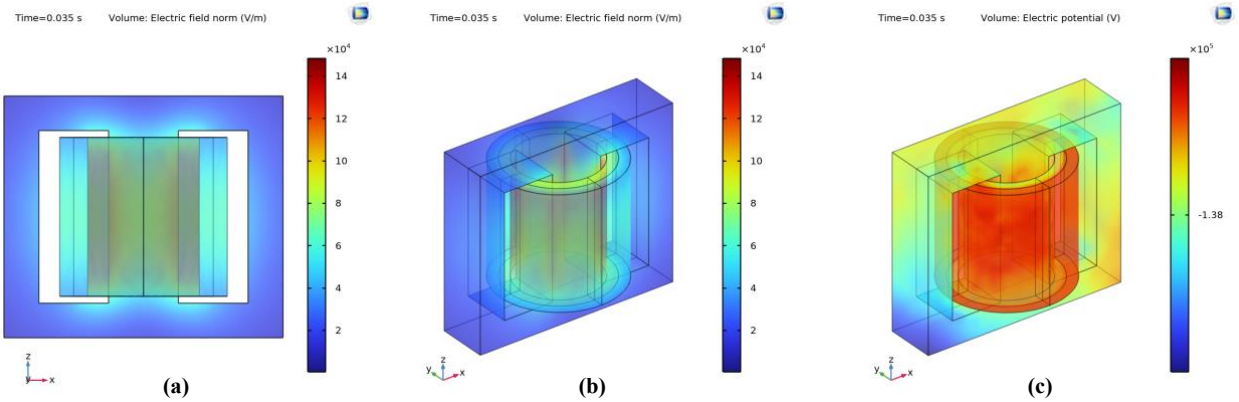

Figure 16. *(a) electric field distribution (xz plane view), (b) electric field distribution (isometric view), (c) electric potential distribution obtained for t=35 ms.*

The magnetic flux density distribution obtained for the composite voltage signal at t=40 ms is given in Figure 17. Due to the decrease in the peak value of the composite voltage signal at t=10 μs, the magnetic flux density, electric field strength, and electric potential in the transformer volume decreased. For this time value, the magnetic flux density was obtained as 0.0986952 T.

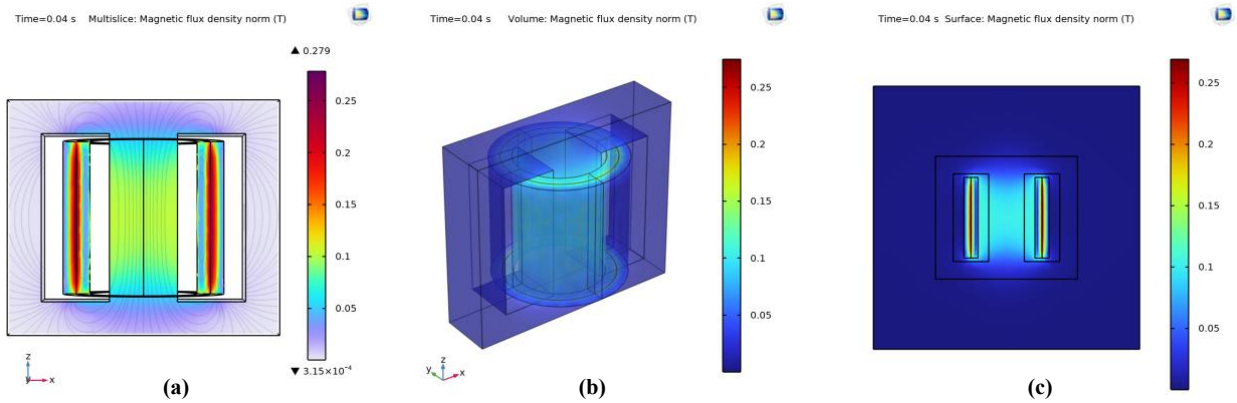

Figure 17. *Magnetic flux density obtained at t=40ms: (a) in the cross-section, (b) in the volume, (c) on the surface.*

The electric field and electric potential distribution obtained for t=40 ms are shown in Figure 18. Due to the decrease in the amplitude of the composite voltage, the electric field strength was obtained as 129.412 V/m. The electric potential distribution obtained for t=40 ms is almost zero in all regions for the transformer volume.

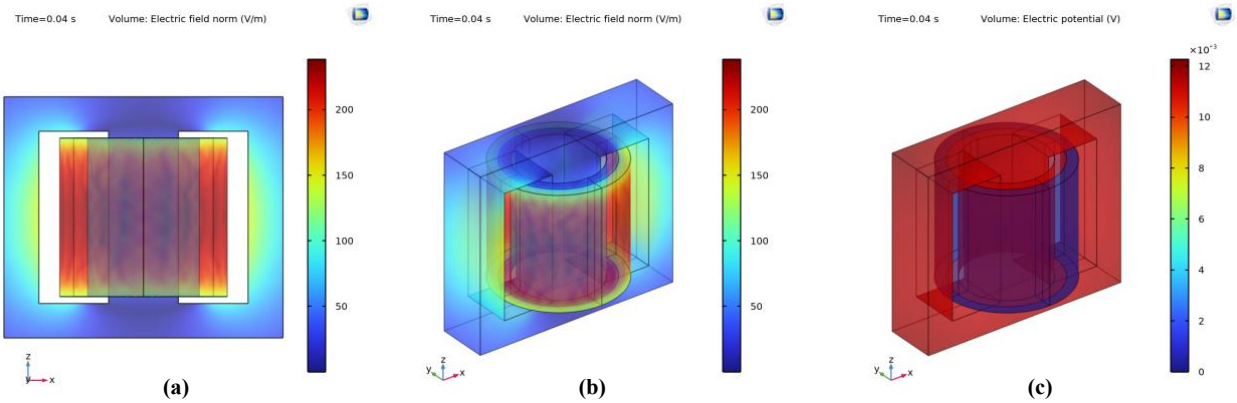

Figure 18. *(a) electric field distribution (xz plane view), (b) electric field distribution (isometric view), (c) electric potential distribution obtained for t=40 ms.*

The magnetic flux density results for the peak value of the nominal operating voltage of the designed transformer are presented in Figure 19. As a result of the analysis performed at t = 45 ms, the maximum magnetic flux density observed in the transformer volume was obtained as 1.15711 T.

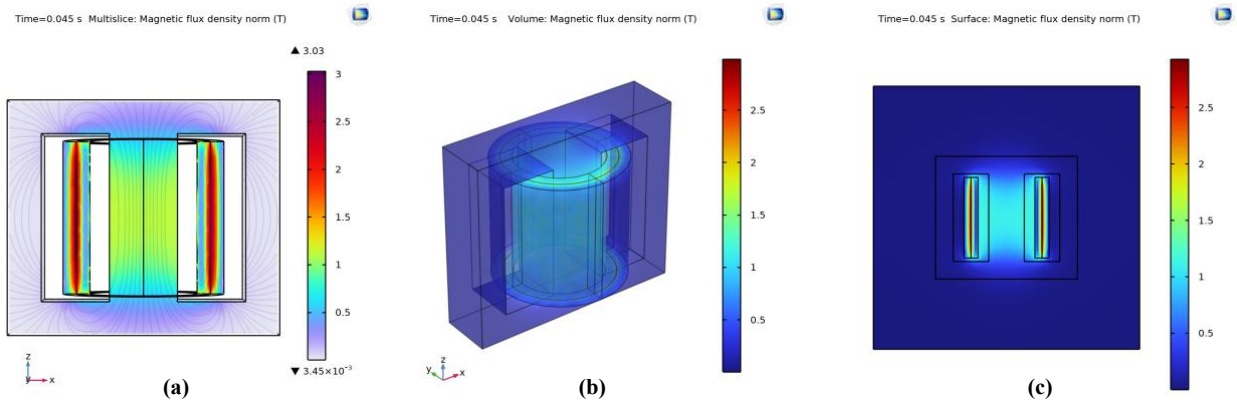

Figure 19. *Magnetic flux density obtained at t=45ms: (a) in the cross-section, (b) in the volume, (c) on the surface.*

The electric field and electric potential distribution at t=45 ms are shown in Figure 20. At the peak value of the nominal operating voltage, the maximum electric field strength was obtained as 18854.7 V/m. The electric potential is uniformly distributed on the surface of the transformer.

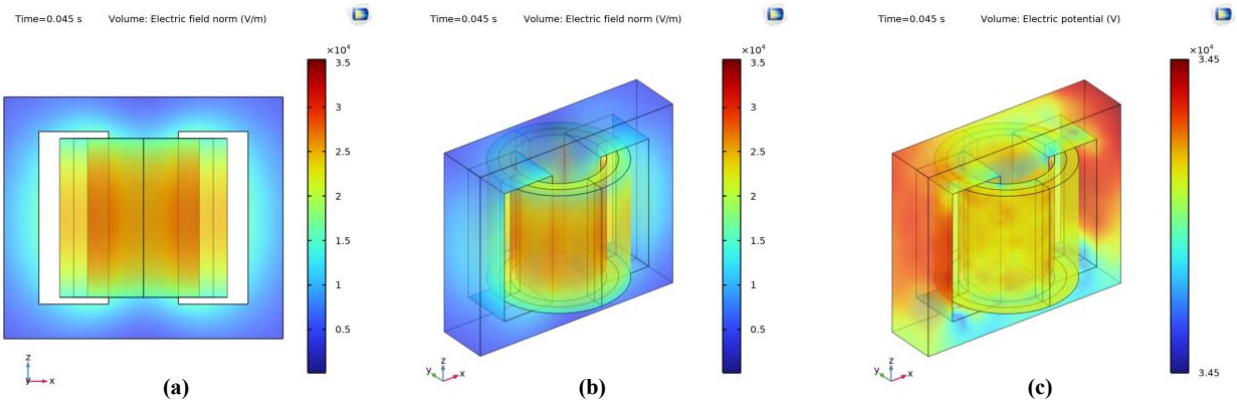

Figure 20. *(a) electric field distribution (xz plane view), (b) electric field distribution (isometric view), (c) electric potential distribution obtained for t=45 ms.*

B. COMPARISON OF THE RESULTS OBTAINED

A composite voltage signal was applied to the high voltage windings of the transformer model designed in COMSOL Multiphysics. In order to analyze the magnetic flux density, electric field distribution, and electric potential over the volume of the transformer, the composite voltage signal was analyzed at six different time moments. The six different time moments were chosen by considering the positive and negative impulse voltage at the positive half-cycle of the nominal operating voltage, the positive and negative impulse voltage at the negative half-cycle of the nominal operating voltage, the zero crossing point of the nominal operating voltage and the maximum value of the nominal operating voltage in the positive region. The signals applied to the designed transformer and the results obtained are presented in Table 2.

Table 2. *Signals applied to the high voltage windings of the designed transformer and the analysis results obtained*

Applied Signal	**Analysis Time**	**Maximum Magnetic Flux Density (T)**	**Maximum Electric Field Strength (V/m)**	**Electric Potential (V)**
Positive Half Cycle Positive Impulse	t= 5 ms	1,82353	78436,2	138445
Negative Half Cycle Positive Impulse	t= 15 ms	1,60468	42343,2	69469,1
Positive Half Cycle Negative Impulse	t= 25 ms	1,59325	- 39690,8	-69467
Negative Half Cycle Negative Impulse	t= 35 ms	1,86759	-79481,2	-138469
Nominal Operating Voltage (Zero Crossing Point)	t= 40 ms	0,0986952	129,412	0,0111031
Nominal Operating Voltage (Positive Peak Value)	t= 45 m	1,15711	18854,7	34500

As a result of the analysis performed in COMSOL Multiphysics software, the magnetic and electrical behavior of the designed transformer under composite voltage signal is presented in Table 1. At t = 5 ms, when the positive impulse voltage reaches its peak value, the magnetic flux density is 1.82353 T, the maximum electric field strength is 78436.2 V/m and the maximum electric potential is 138445 V. These results show the effect of the impulse voltage on the magnetic core of the transformer and the increase in the electric field distribution.

In the region where the positive impulse voltage is applied in the negative half-cycle, the maximum magnetic flux density is 1.60468 T, the maximum electric field strength is 42343.2 V/m and the maximum electric potential is 69469.1 V for the peak value of the composite voltage at t = 15 ms. These results show the effect of the positive impulse in the negative half-cycle on the transformer volume.

At t=25 ms, a negative electric field strength of 39690.8 V/m was formed on the transformer due to the effect of the negative impulse voltage on the positive half-cycle of the operating voltage. The maximum amplitude value of the electric potential on the transformer was 69467.

At the time t=35 ms, the results are very similar to those obtained at the time t=5 ms for the negative impulse voltage at the negative half cycle of the AC. At this moment, the magnetic flux density on the transformer volume is 1.86759 T and the amplitude of the electric field strength is 18854.7 V/m. The slight difference observed between the magnetic flux densities for the positive and negative half-cycle impulse voltages (1.82353 T vs. 1.86759 T) is attributed to the nonlinear and asymmetric behavior of the transformer core material. Due to the hysteresis effect and structural asymmetries within the core, the magnetic saturation point can vary depending on the direction of the applied magnetic field. This phenomenon is supported by the work of Aboura et al. [29], where hysteresis-based modeling showed similar deviations in flux density under polarity changes.

A significant decrease in magnetic flux density, electric field, and potential magnitudes was observed at t = 40 ms corresponding to the zero crossing point of the nominal operating voltage. At this time, the magnetic flux density is 0.0986952 T, the maximum electric field strength is 129.412 V/m and the electric potential is 0.0111031 V. This indicates that the decrease in the composite voltage amplitude affects the magnetic and electrical parameters of the transformer significantly.

Finally, at t = 45 ms, when the nominal operating voltage reaches its peak value, the magnetic flux density is 1.15711 T, the maximum electric field strength is 18854.7 V/m and the electric potential is 34500 V. It was observed that the electric potential distribution is uniform over the transformer surface for t = 45 ms.

The findings of this study reveal notable increases in both electric field intensity and magnetic flux density under composite voltage conditions. The electric field rose from 18,854.7 V/m during normal operation to 78,436.2 V/m under transient stress, while the magnetic flux density increased from 1.15711 T to 1.82353 T. Similar behavior was reported by Özüpak, who investigated a 33/11 kV dry-type transformer subjected to a 1000 kV lightning impulse. In that study, the electric field increased from 0.85×10^{2} V/m to 1.45×10^{5} V/m, and the magnetic flux density from 1.84 T to 3.64 T. These results confirm that significant rises in electromagnetic parameters are typical under high-stress conditions such as lightning surges or switching events. The consistency between the outcomes of this study and those found in the literature supports the reliability of the simulation model and underlines the importance of accounting for such extreme conditions in transformer design and insulation analysis.

IV. CONCLUSION

In this study, a detailed analysis of the magnetic flux density, electric field strength, and electric potential distribution of a 3 MVA distribution transformer under a composite voltage signal is carried out. The analyses performed using COMSOL Multiphysics software are expected to make a significant contribution to the literature on the behavior of transformers under composite voltage conditions.

The results show that the lightning impulse voltage causes electrical stress on the transformer insulation system. It was found that the maximum magnetic flux density increased by 57.59% and the maximum electric field strength was 316% higher for positive impulse voltage at positive half-cycle compared to nominal operating conditions. a In addition, composite voltage signals with a larger amplitude impulse voltage component are known to stress transformers even more in terms of electric field strength and magnetic flux density. This plays a critical role in understanding the potential causes of dielectric breakdown and thermal stresses in the insulating material.

Consequently, such analysis under composite voltages is critical for the safe and efficient operation of transformers. It is expected that these analyses will contribute to the understanding of the factors affecting the insulation system by providing important data for the evaluation of insulation and safety criteria in transformer design. Furthermore, the proposed COMSOL Multiphysics model allows researchers and engineers to simulate a range of voltage stress scenarios that go beyond traditional AC or impulse-only testing. This enables the development and testing of new insulation design strategies without the need for immediate physical prototyping. The modular nature of the model supports its expansion with different voltage types, material properties, and transformer configurations, enhancing its potential contribution to the transformer insulation literature.

In addition to providing a detailed analysis of the transformer under composite voltage conditions, the presented simulation model can serve as a foundational reference for evaluating insulation performance under multiple types of stress. By modifying the waveform parameters or transformer geometry, the model can be adapted for different transformer types and stress scenarios. This flexibility positions the model as a potential base for future studies aiming to develop advanced insulation structures or to evaluate the aging characteristics of insulation under complex voltage conditions. In addition, the obtained results are valid for the simulated 3 MVA, 34.5 kV dry-type distribution transformer and can be considered as a reference for transformers with similar design and voltage levels. However, variations in transformer structure, insulation material, or applied voltage waveform may result in different outcomes. Therefore, testing the model under different configurations would help to improve the generalizability of the results.

Future studies may extend the current analysis by incorporating different impulse waveforms (such as switching surges), temperature variations, or environmental factors like humidity. Coupling electromagnetic and thermal analyses could also provide deeper insight into long-term insulation performance, thus supporting the development of more robust transformer designs.

Article Information

Acknowledgments: The authors would like to express their sincere thanks to the editor and the anonymous reviewers for their helpful comments and suggestions.

Author's Contributions: Writing—original draft, E.T. and M.F., writing—review, analysis and editing, E.T., M.F.. All authors have read and approved the final version of it.

Artificial Intelligence Statement: No any Artificial Intelligence tool is used in this paper.

Conflict of Interest Disclosure: No potential conflict of interest was declared by authors.

Plagiarism Statement: This article was scanned by the plagiarism program.

V. REFERENCES

[1] J. Sun, Q. Yang, P. Su, S. Wu, S. Chen and L. He, "Diagnosis of winding fault in three-winding transformer using lightning impulse voltage," *Electric Power Systems Research*, vol. 175, 2019, Art. no. 105898.

[2] X. Zhang, H. Wang, R. Guo, Z. Zhang, J. Li and X. Han, "Fault diagnosis technologies for power transformers during the on-site inductive oscillating switching impulse voltage withstand test," *IET Generation, Transmission and Distribution*, vol. 16, no. 19, pp. 3894–3905, 2022.

[3] M. Florkowski, J. Furgal, M. Kuniewski and P. Pajak, "Comparison of transformer winding responses to standard lightning impulses and operational overvoltages," *IEEE Transactions on Dielectrics and Electrical Insulation*, vol. 25, no. 3, pp. 965–974, 2018.

[4] E. Tunç and M. Fidan, "Residual Voltage Tests of 4.5 kV Metal Oxide Surge Arrester," in *2023 14th International Conference on Electrical and Electronics Engineering (ELECO)*, Bursa, Türkiye, 2023, pp. 1-5.

[5] R. R. Annadi and C. S. Patsa, "Estimation of switching surge flashover rate of 1200-kV UHVAC transmission line considering switching overvoltage waveshape," *Electrical Engineering*, vol. 102, no. 2, pp. 953–966, 2020.

[6] Y. Zheng, B. Yu, H. Xu, D. Yan, X. Li and W. He, "Novel method for restraining 35 kV shunt reactor switching overvoltage – phase controlled breaker," *The Journal of Engineering*, vol. 2019, no. 16, pp. 742–747, 2019.

[7] E. Tunc and M. Fidan, "Experimental and simulation study of pulse current generator," *Electric Power Components and Systems*, vol. 52, no. 8, pp. 1316–1327, 2024.

[8] L. F. Freitas-Gutierres et al., "Framework for decision-making in preventive maintenance: Electric field analysis and partial discharge diagnosis of high-voltage insulators," *Electric Power Systems Research*, vol. 233, 2024, Art. no. 110447.

[9] M. Fidan and H. İsmailoğlu, "$CuSO_45H_2O$ sıvı direncin harmonikli ve harmoniksiz yüksek gerilim altında kismi boşalma davranışları," *Journal of the Faculty of Engineering and Architecture of Gazi University*, vol. 32, no. 1, pp. 315–323, 2017.

[10] Y. Özüpak, "Ansys@maxwell kullanılarak transformatörlerin ani akımlar durumunda meydana gelen elektrik alan analizlerinin gerçekleştirilmesi," *Adıyaman Üniversitesi Mühendislik Bilimleri Dergisi*, vol. 8, no. 14, pp. 105–116, 2021.

[11] *Power Transformers - Part 3: Insulation Levels, Dielectric Tests and External Clearances in Air*, IEC 60076-3:1980, Geneva, Switzerland, 1980. [Online]. Available: https://forhandsvis.standard.no/product/1890428/en.

[12] Y. Özüpak and E. Aslan, "Using artificial neural networks to improve the efficiency of transformers used in wireless power transmission systems for different coil positions," *Revue Roumaine des Sciences Techniques, Série Électrotechnique et Énergétique*, vol. 69, pp. 195–200, 2024.

[13] Y. Özüpak and M. S. Mamiş, "Analysis of electromagnetic and loss effects of sub-harmonics on transformers by Finite Element Method," *Sādhanā*, vol. 45, 2020, Art. no. 226.

[14] R. Hu, Z. Zhang, S. Wang, Y. Lu, L. Liu and S. Zhu, "Electric field optimization of cast resin dry-type transformer under lightning impulse," in *Conference on Electrical Insulation and Dielectric Phenomena, (CEIDP)*, IEEE, Richland, WA, Washington, USA, 2019, pp. 556-559.

[15] M. M. Ispirli, B. Oral and Ö. Kalenderli, "Electric field analysis of 66 kV and 110 kV SiR insulators under combined AC–DC voltages," *Energy Reports*, vol. 8, pp. 361–368, 2022.

[16] M. Yazici, Ö. Kalenderli and M. M. Ispirli, "Simulation of the composite electric field on 170 kV disconnector using the finite-element method," *Electrica*, vol. 24, no. 1, pp. 87–95, 2024.

[17] M. S. Seddik, J. Shazly and M. B. Eteiba, "Thermal analysis of power transformer using 2D and 3D finite element method," *Energies*, vol. 17, no. 13, 2024, Art. no. 3203.

[18] M. A. Tsili, E. I. Amoiralis, A. G. Kladas and A. T. Souflaris, "Power transformer thermal analysis by using an advanced coupled 3D heat transfer and fluid flow FEM model," *International Journal of Thermal Sciences*, vol. 53, pp. 188–201, 2012.

[19] *High-Voltage Test Techniques- Part 1: General Definitions and Test Requirements*, "IEC 60060-1:2010-," Geneva, Switzerland, 2010. [Online]. Available: https://cdn.standards.iteh.ai/samples/14599/5b8e92914b8b41c1a2d22e6ea9fbabb3/IEC-60060-1-2010.pdf.

[20] X. Meng, X. Li and T. Lu, "Statistical properties of corona current pulses in rod-plane air gap under AC-DC composite voltages," *IEEE Transactions on Dielectrics and Electrical Insulation*, vol. 31, no. 1, pp. 212–221, 2024.

[21] J. Jiang, W. Liu, Z. Li, Z. Shen and C. Zhang, "Partial discharge characteristics of aviation cables under composite voltages," *IEEE Transactions on Dielectrics and Electrical Insulation*, vol. 31, no. 3, pp. 1193–1200, 2024.

[22] S. Dedeoglu and A. Merev, "Realization of the reference composite voltage waveforms for lightning impulse (LI) voltages superimposed over DC and AC signals," *Mapan - Journal of Metrology Society of India*, vol. 38, no. 3, pp. 597–606, 2023.

[23] M. M. Ispirli, Ö. Kalenderli, F. Seifert, M. Rock and B. Oral, "Investigation of impact of DC component on breakdown characteristics for different electric fields under composite AC & DC voltage," *High Voltage*, vol. 7, no. 2, pp. 279–287, 2022.

[24] P. Sun, W. Sima, M. Yang, X. Lan and J. Wu, "Study on voltage-number characteristics of transformer insulation under transformer invading non-standard lightning impulses," *IEEE Transactions on Dielectrics and Electrical Insulation*, vol. 22, no. 6, pp. 3582–3591, 2015.

[25] P. K. Samaras, E. T. Staikos, Z. G. Datsios, P. N. Mikropoulos, T. E. Tsovilis and N. D. Kokkinos, "Evaluation of the electric stress on an insulating down-conductor caused by lightning strikes through ATP-EMTP simulations," *IEEE Transactions on Industry Applications*, vol. 60, no. 6, pp. 8353-8361, 2024.

[26] *High-Voltage Test Techniques - Part 2: Measuring Systems*, IEC 60060-2:2010, Geneva, Switzerland, 2010. [Online]. Available: https://cdn.standards.iteh.ai/samples/15064/134aee6cd6844b35b2469fd5826964e4/IEC-60060-2-2010.pdf.

[27] *High-Voltage Test Techniques - Part 3: Definitions and Requirements for on-Site Testing*, IEC 60060-3:2006, Geneva, 2006. [Online]. Available:

https://cdn.standards.iteh.ai/samples/1000002023/8302a36ea68d469e988a72f714da3426/IEC-60060-3-2006.pdf.

[28] Ö. Kalenderli, E. Ok and S. Çelebi, "14 kV luk Darbe Gerilimi Üreteci Tasarımı ve Yapımı," 2009. [Online]. Available: https://www.emo.org.tr/ekler/01cfd14f121f19b_ek.pdf.

[29] F. Aboura and O. Touhami, "Integration of the hysteresis in models of asymmetric three-phase transformer: Finite-element and dynamic electromagnetic models," *IET Electric Power Applications*, vol. 10, no. 7, pp. 614–622, 2016.